JMB

Available online at www.sciencedirect.com

ScienceDirect

ELSEVIER

Conformational Dynamics of the Molecular Chaperone Hsp90 in Complexes with a Co-chaperone and Anticancer Drugs

Jonathan J. Phillips[1,2], Zhong-ping Yao[1], Wei Zhang[2]
Stephen McLaughlin[1,2], Ernest D. Laue[2], Carol V. Robinson[1]
and Sophie E. Jackson[1]*

[1]*Cambridge University Chemical Laboratory University of Cambridge Lensfield Road, Cambridge CB2 1EW, UK*

[2]*Department of Biochemistry University of Cambridge Old Addenbrookes Site 80 Tennis Court Road Cambridge, CB2 1GA, UK*

*Corresponding author

The molecular chaperone Hsp90 is essential for the correct folding, maturation and activation of a diverse array of client proteins, including several key constituents of oncogenic processes. Hsp90 has become a focus of cancer research, since it represents a target for direct prophylaxis against multistep malignancy. Hydrogen-exchange mass spectrometry was used to study the structural and conformational changes undergone by full-length human Hsp90β in solution upon binding of the kinase-specific co-chaperone Cdc37 and two Hsp90 ATPase inhibitors: Radicicol and the first-generation anticancer drug DMAG. Changes in hydrogen exchange pattern in the complexes in regions of Hsp90 remote to the ligand-binding site were observed indicating long-range effects. In particular, the interface between the N-terminal domain and middle domains exhibited significant differences between the apo and complexed forms. For the inhibitors, differences in the interface between the middle domain and the C-terminal domain were also observed. These data provide important insight into the structure of the biologically active form of the protein.

© 2007 Elsevier Ltd. All rights reserved.

Keywords: Hsp90; co-chaperone; hydrogen exchange mass spectrometry; anti-cancer drugs

Introduction

Heat shock protein 90 (Hsp90) is an essential molecular chaperone in eukaryotic cells. As a chaperone it is unique in its functions as it is not required for the maturation or maintenance of most proteins *in vivo*, but has a specific set of client or substrate proteins. It plays a critical and central role in the assembly and maturation pathways of a number of important cellular complexes, many of which are involved in signal transduction path-

ways.[1,2] It is thought that the role of Hsp90 is to keep the client proteins poised for activation until they are stabilised either by a conformational change or by binding of a cofactor, ligand or partner protein.[3]

Hsp90 does not act alone but works alongside a cohort of co-chaperone proteins that includes Hsp40, Hsp70, HOP, Cdc37, p23, and high molecular weight immunophilins.[1] Recent work mapping the proteins that interact either physically or genetically with Hsp90 in *Saccharomyces cerevisiae* has established that there are many more, as yet uncharacterised, potential co-chaperones.[2] In some cases, the role of these co-chaperones is clear; for example, Hsp40, Hsp70 and HOP act together to present the client protein to Hsp90.[4] In other cases, their roles are much less well defined. Together, Hsp90 and co-chaperones constitute a cellular assembly machine.

Hsp90 has a weak, but essential, ATPase activity and mutants of Hsp90 with hyper or hypo activity have compromised function *in vivo*.[5] Many of the co-chaperones are known to regulate this ATPase

activity.[6–11] Several different classes of small molecules have been identified or developed in the past ten years that bind to and inhibit the ATPase activity of Hsp90. These include natural products such as the ansamycin family,[12] which includes geldanamycin and derivatives thereof, the macrolide inhibitor radicicol,[13] and designed purine-based drugs.[14] These inhibitors have been shown to possess potent anti-tumour activity *in vitro* and are now being widely developed as cancer chemotherapeutics. Recent results of Phase I clinical trials have established the proof-of-principle for these types of drugs and Phase II clinical trials are currently underway focussing on specific malignancies.[15–17]

Hsp90 has three major structural domains, the N-terminal domain (NTD) that contains the ATP and inhibitor-binding site and which also binds to co-chaperones such as Cdc37 and p23; the middle domain (MD), which is thought to constitute the main client protein binding site and encompass the binding site of the co-chaperone Aha1; and the C-terminal domain (CTD), which contains the dimerisation interface (Figure 1). Hsp90 is a symmetric homo-dimer; also in the C-terminal domain is a MEEVD motif that is responsible for the binding of co-chaperones that contain a TPR domain. Structures for the isolated, individual domains have been reported either for human or yeast Hsp90, the ER homologue Grp94 or the *Escherichia coli* homologue, HtpG.[18–24] In addition, a number of structures of larger constructs have been reported including the NTD and middle domain of HtpG,[25] and recently full-length HtpG[26] and an engineered variant of full-length yeast Hsp90 complexed with nucleotide and p23.[27]

The structures, in combination with kinetic studies on wild-type and mutant Hsp90s, have provided some insight into the action of Hsp90.[28] A number of studies support a model in which there is a dimerisation of the N-terminal domains on ATP binding leading to a closed, cyclised structure;[18,29,30] it was thought that the client protein was encapsulated in the centre of the molecular clamp, however, recent crystal structures have shown that there is insufficient space for most client proteins.[27] In contrast, other studies have shown that the two ATP-binding and hydrolysis sites in human Hsp90, in the absence of co-chaperones, can act independently and show no evidence for N-terminal dimerisation.[31]

Although the crystal structures have provided much important information on Hsp90, in many cases they only provide information on a single isolated domain. In addition, they represent a snapshot of the system in a single, trapped conformation in the crystalline form. Here, we have used a complementary approach using H/D exchange techniques, in conjunction with mass spectrometric analysis, in order to obtain information on the conformational changes that are induced in full-length Hsp90 on binding inhibitors and co-chaperones. It should be stressed that in contrast to the crystal structures, these measurements are made in solution and may, therefore, give a more accurate view of the molecule as it

functions *in vivo*. We have chosen two systems to study in detail: complexes of Hsp90 with the anti-tumour agents geldanamycin and radicicol, as well as the complex of Hsp90 with the kinase-specific co-chaperone Cdc37. In the first case, crystal structures for the inhibitors bound to the N-terminal domain of Hsp90 are known,[20,21] but these do not provide information on the effect of inhibitor binding on the middle or C-terminal domains. We have evidence from small angle X-ray scattering (SAXS) studies, that geldanamycin induces a change in the ensemble of structures adopted by free Hsp90, which results in an overall compaction of the protein.[6] Using H/D exchange (HX) and MS techniques we are able to locate regions of the protein that become more or less structured. A crystal structure for the complex formed between the C-terminal segment of human Cdc37 (from residue 148 to 347) and the N-terminal domain of yeast Hsp90 exists,[32] but again, this provides little information on the long-range effects of binding Cdc37 to Hsp90. We have also investigated this interaction by HX-MS techniques. In both cases, binding of ligands to the N-terminal domain induces conformational changes in the middle and C-terminal domains, indicating that there is significant communication between domains and long-range effects of both small molecule inhibitor and co-chaperone binding. The consequences of these results for the mechanism of Hsp90 are discussed.

Results and Discussion

We have investigated and report here the results of H/D exchange mass spectrometric analysis of three complexes of full-length human Hsp90β: with a water-soluble derivative of 17-dimethylaminoethyl-amino-17-demethoxygeldanamycin (DMAG), radicicol (RD) and the minimal Hsp90-binding domain of the co-chaperone Cdc37 (this comprises the central domain from residue 147 to 276 and which we refer to here as Cdc37c).

Sequence assignment

Prior to the hydrogen-exchange experiments, non-deuterated Hsp90 was digested for assignment of peptic peptides to the primary sequence. Due to the notably large size of the system being studied (a dimer of a 90 kDa polypeptide) the digest spectra were extremely complex with many overlapping series of ions; a typical spectrum for the peptic digestion products of Hsp90 is shown in Figure 2(a). As is evident from the inset panel, which shows an expanded view of one region of the spectrum, the high resolution that was achieved with nano-ESI-MS enabled even overlapping species to be resolved and identified correctly. Each peptide ion was subjected to MS/MS for sequence assignment and 72 peptide ions were identified, some of which belong to the same peptides but in different charge states and are, thus, degenerate. Other peptide ions were from partially overlapping regions of the sequence and
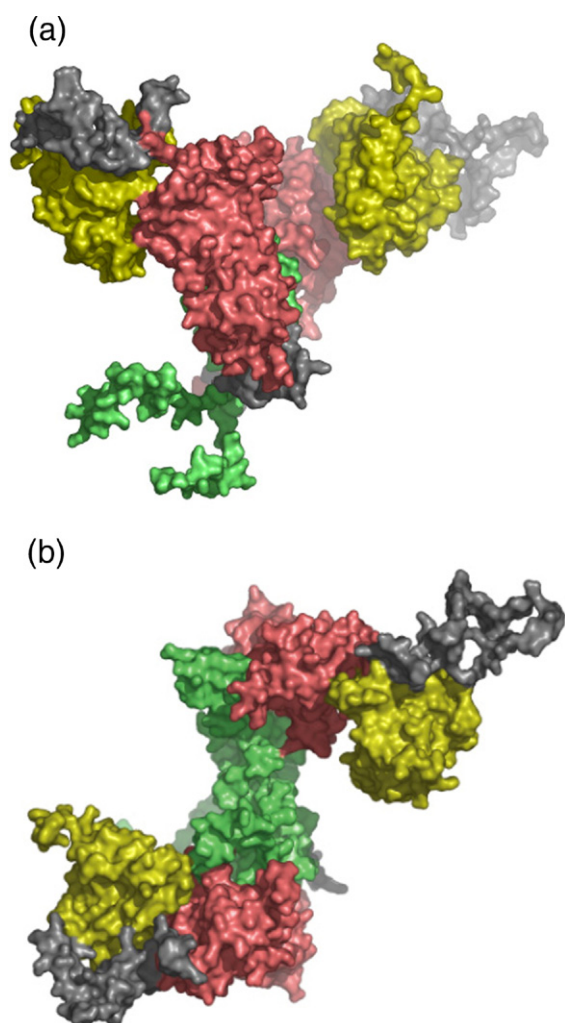
(a)

(b)

Figure 1. Orthogonal views of the comparative model of human Hsp90β. Surface model is shown, coloured by structured domains for each of the two monomers: NTD, yellow; middle domain, red; and CTD, green. Unstructured regions are coloured grey.

these serve to increase the net resolution of the data. Rather poor coverage in the charged linker region was observed, which may be due to its highly degenerate sequence, rendering it particularly difficult to assign unique peptides to. It is also probable that its lack of stable structure means it was more fully proteolysed by pepsin than were other regions. The total sequence coverage of human Hsp90β was 68% of the structured regions: 56% of the NTD, 66% of the middle domain and 72% of the CTD (Figure 3).

H/D exchange experiments on complexes of Hsp90

HX-MS data were acquired for the unliganded Hsp90 dimer and the three complexes: Hsp90-DMAG, Hsp90-RD and Hsp90-Cdc37c; Figure 2(b) shows typical raw data. Two types of measurements are made:(i) on-exchange in which the number of protons that exchange with solvent deuterons is de-

termined for each peptide, and (ii) off-exchange in which the exchange of deuterated amide groups with solvent protons is followed over a time-course. For off-exchange, the rates were classified into one of three regimes, fast, intermediate and slow. Figure 4 shows the data for each peptide measured, for free Hsp90 and the Hsp90-inhibitor complexes, superimposed on the structure of Hsp90. The peptides are colour-coded: the slowest observed hydrogen-exchange rates are shown in blue, intermediate rates in magenta and fast rates in red. Yellow indicates a peptide that does not undergo any off-exchange over the time-course of the experiment. The zero-time point data indicate the maximum detectable on-exchange (where deuterium exchanges onto the protein) for each peptide during the overnight equilibration period prior to initiating off-exchange of the amide-deuterium for hydrogen. This initial data point accounts for the degree of off-exchange that occurs upon acid-quenching and aqueous pepsin-digest of the protein. Data for each of the complexes were compared with free Hsp90 and changes in either the H/D exchange patterns or rates noted, thereby establishing the regions of Hsp90 that become more or less structured or accessible to solvent on complex formation.

Conformational changes in Hsp90 upon inhibitor binding

Regions of Hsp90 that show significant differences in their H/D exchange patterns and/or rates on DMAG or RD binding, indicative of conformational change, are discussed in detail below domain by domain. The conformational changes may be due to a local change in structure or a change in the quaternary structure of the protein that leads to a change in solvent accessibility of the backbone amide groups.

The N-terminal domain

The NTD of Hsp90 adopts a Bergerat fold and has an eight-stranded β-sheet, of which seven strands are antiparallel and the terminal strand (β8) is parallel. The sheet is flanked on one face by helices that form a unique ATP-binding pocket and a lid segment comprising the three helices α5, α6 and α7. The lid segment rotates relative to the plane of the β-sheet upon nucleotide or inhibitor binding to the adjacent pocket.[19–21] In high-resolution models of the multi-domain constructs of Hsp90 that include the NTD, there are multiple possible sites of interaction between the NTD and the middle domain and between the NTD of each monomer upon the formation of an N-terminally cyclised Hsp90 dimer.[24–27,30]

Figure 5(a) illustrates the pattern of hydrogen-exchange that we observe throughout the NTD of the full-length Hsp90 dimer in the free and liganded states. From these data, it is not only possible to obtain information on the conformational changes induced on inhibitor binding within the NTD but also changes in inter-domain interactions.
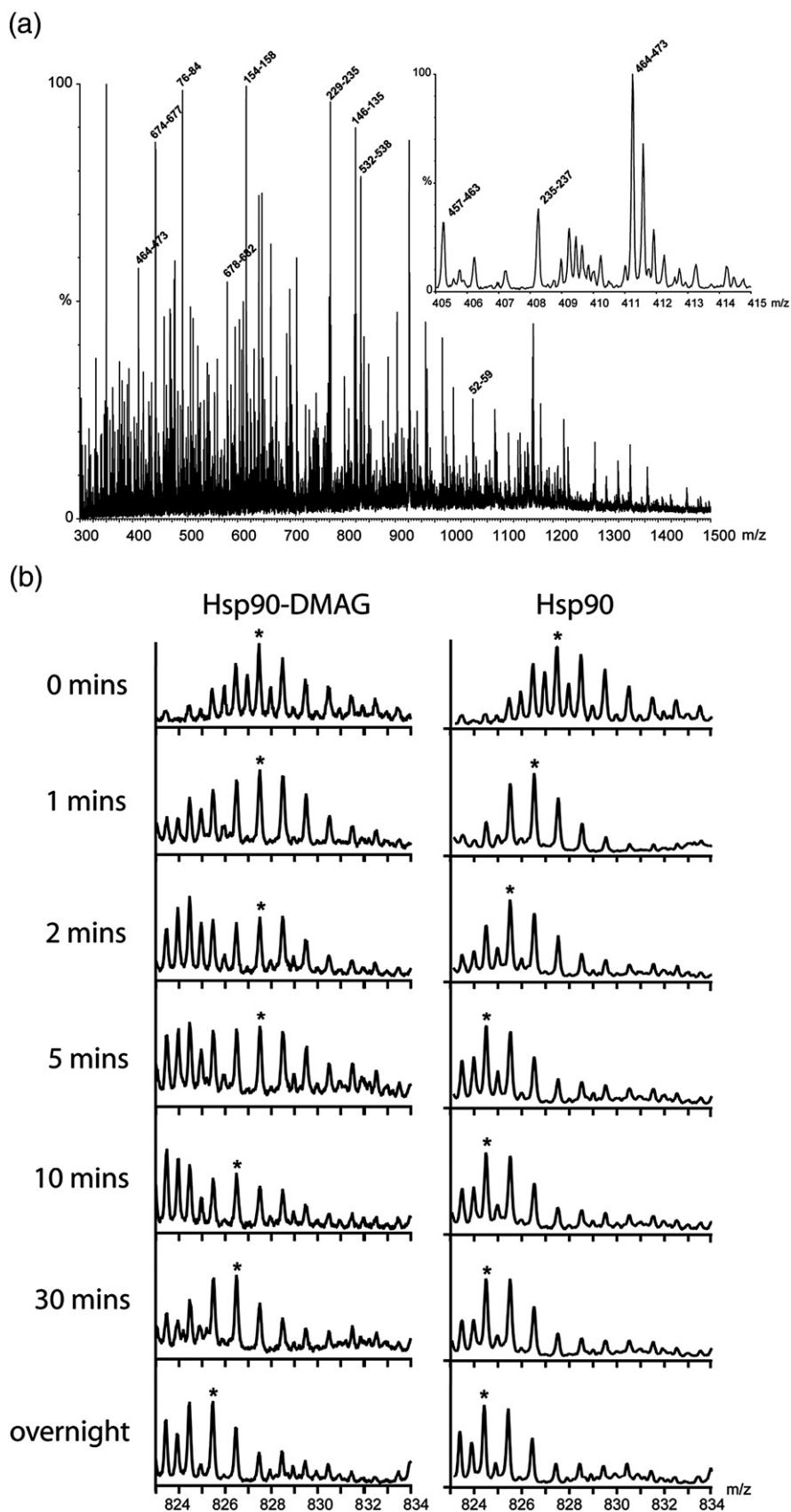
Figure 2. (a) A typical mass spectrum for the pepsin digest of Hsp90. Shown are data averaged from 1 min of acquisition by nano-ESI-MS. Inset is an enlargement of the region for 405–415 *m/z*, which highlights the near-baseline resolution of triply charged ions in the spectrum and also the overlapping series of ions that contribute to the complexity of analysis. (b) H/D exchange results for the charged peptide ion 824.42 (residues 146–153) in the free Hsp90 dimer and in the Hsp90-DMAG complex.
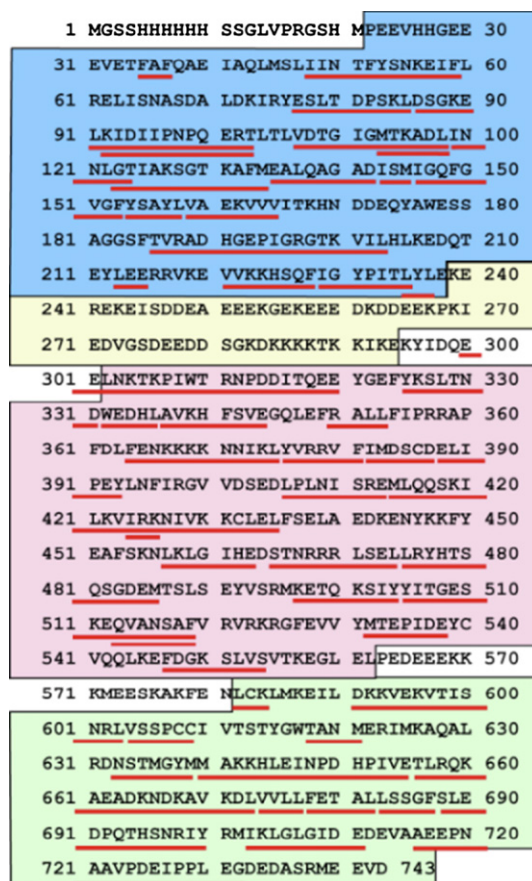
```
  1 MGSSHHHHHH SSGLVPRGSH MPEEVHHGEE  30
 31 EVETFAFQAE IAQLMSLIIN TFYSNKEIFL  60
 61 RELISNASDA LDKIRYESLT DPSKLDSGKE  90
 91 LKIDIIPNPQ ERTLTLVDTG IGMTKADLIN 100
121 NLGTIAKSGT KAFMEALQAG ADISMIGQFG 150
151 VGFYSAYLVA EKVVVITKHN DDEQYAWESS 180
181 AGGSFTVRAD HGEPIGRGTK VILHLKEDQT 210
211 EYLEERRVKE VVKKHSQFIG YPITLYLEKE 240
241 REKEISDDEA EEEKGEKEEE DKDDEEKPKI 270
271 EDVGSDEEDD SGKDKKKKTK KIKEKYIDQE 300
301 ELNKTKPIWT RNPDDITQEE YGEFYKSLTN 330
331 DWEDHLAVKH FSVEGQLEFR ALLFIPRRAP 360
361 FDLFENKKKK NNIKLYVRRV FIMDSCDELI 390
391 PEYLNFIRGV VDSEDLPLNI SREMLQQSKI 420
421 LKVIRKNIVK KCLELFSELA EDKENYKKFY 450
451 EAFSKNLKLG IHEDSTNRRR LSELLRYHTS 480
481 QSGDEMTSLS EYVSRMKETQ KSIYYITGES 510
511 KEQVANSAFV RVRKRGFEVV YMTEPIDEYC 540
541 VQQLKEFDGK SLVSVTKEGL ELPEDEEEKK 570
571 KMEESKAKFE NLCKLMKEIL DKKVEKVTIS 600
601 NRLVSSPCCI VTSTYGWTAN MERIMKAQAL 630
631 RDNSTMGYMM AKKHLEINPD HPIVETLRQK 660
661 AEADKNDKAV KDLVVLLFET ALLSSGFSLE 690
691 DPQTHSNRIY RMIKLGLGID EDEVAAEEPN 720
721 AAVPDEIPPL EGDEDASRME EVD 743
```

Figure 3. Sequence coverage map for the peptic peptide assignment of human Hsp90β. Each assigned peptide is depicted as a red bar underneath the corresponding stretch of sequence. Domains of Hsp90 are coloured: blue, NTD; yellow, charged linker; pink, middle domain; and green, CTD.

For both the RD and DMAG complexes, clear differences in the protection of amides are observed in the ATP-binding site, as probed by peptide ion 824.42 (Figures 2(b) and 5(a)). This peptide ion corresponds to an octapeptide (residues 146–153), comprising part of α5 and α6 and the intervening loop, which binds directly to the inhibitory ligands: the phenyl ring of Phe153 makes hydrophobic contacts with the coplanar aromatic ring of RD, analogous to the mode of binding of purines in the active site, and the main-chain N-H of Phe153 hydrogen-bonds to the amide carbonyl of the ansamycins.[21,33] The significant protection of this peptide ion in the inhibitor complexes and the fact that the peptide does not exhibit greater on-exchange in these complexes, suggests that there is no large-scale structural rearrangement in this region on complex formation, but that binding of ligand has occurred.

Peptide ion 776.46 corresponds to a peripheral strand of the β-sheet in the NTD, β8, and the preceding α9-β8 loop that contains residue Phe228, which is known to make a stable interaction with Tyr376 of the middle domain in the Hsp90/AMP-PNP/p23 complex.[27] This peptide exchanges all deuterons within 30 min in the free protein (an intermediate exchange regime), but exchange becomes slow in the presence of DMAG ligand (Figure 5(a)).

HX-MS data were obtained for a tetrapeptide at the C terminus of α1 (peptide ion 460.28) and for three sequential peptides of the lid segment (peptide ions 350.22, 824.42 and 616.38) (Figure 5(a)). There was no difference in the degree of on-exchange (i.e. data for the zero-time points are not significantly different) or in the rate of off-exchange in α1 for Hsp90-DMAG and Hsp90-RD relative to the free dimer. Both detectable amide groups in the tripeptide 350.22 on-exchange with deuterium in the equilibration period, yet there is no discernable off-exchange over 18 h at 25 °C in the inhibitor ligand-bound complexes and only 0.5 deuterons exchanged off in the free protein. α7, which is located underneath the two other helices of the lid-segment, remains equally buried in all liganded states and apo-Hsp90, as shown by the exchange pattern of peptide ion 616.38. The lack of alteration in total on-exchange between the apo (1.3 deuterons), RD-bound (0.9 deuterons) and DMAG-bound (1.1 deuterons) states of Hsp90 indicates that the degree of structure of α6 remains the same for Hsp90, Hsp90-RD and Hsp90-DMAG. Together, these data are consistent with the NTD models presented in Figure 6(a), in which the ligand-bound lid-segment adopts the "open" conformation.

The middle domain

Information on conformational changes in the middle domain on binding of inhibitors to the NTD comes from a number of different peptide ions. These report on the Aha1-binding site and on a possible middle domain–NTD interface involving the catalytic loop. The catalytic loop contains a conserved arginine residue, Arg412 (Arg380 in yeast Hsp82), which orients the γ-phosphate of ATP bound in the NTD for effective hydrolysis.[27] Two peptide ions report on the region encompassing α11 and the preceding β13-α11 loop; peptide ion 875.87 corresponds to a 22mer peptide spanning this region, and the peptide ion 416.30 was assigned to a tripeptide within α11 (Figure 5(b)). In our model of human Hsp90β, and in published models of homologues, α11 is packed against the five-stranded β-sheet[22,23] and makes no contact with the NTD (Figure 1).[25] The putative interaction with the NTD lies entirely within the β13-α11 catalytic loop, for which we have data on five amide groups covered by the 875.87 peptide ion. 10.4 deuterons were incorporated into this peptide in the DMAG complex during the period of on-exchange, an increase of one deuteron compared with the apo-protein, yet two additional amide protons exchanged off under a fast regime. Given that there was no off-exchange in either sample for the 416.30 species (Figure 5(b)), it can be surmised that the increased amide exchange is a result of reduced higher-order structure at the N terminus of α11 or in the preceding loop in the
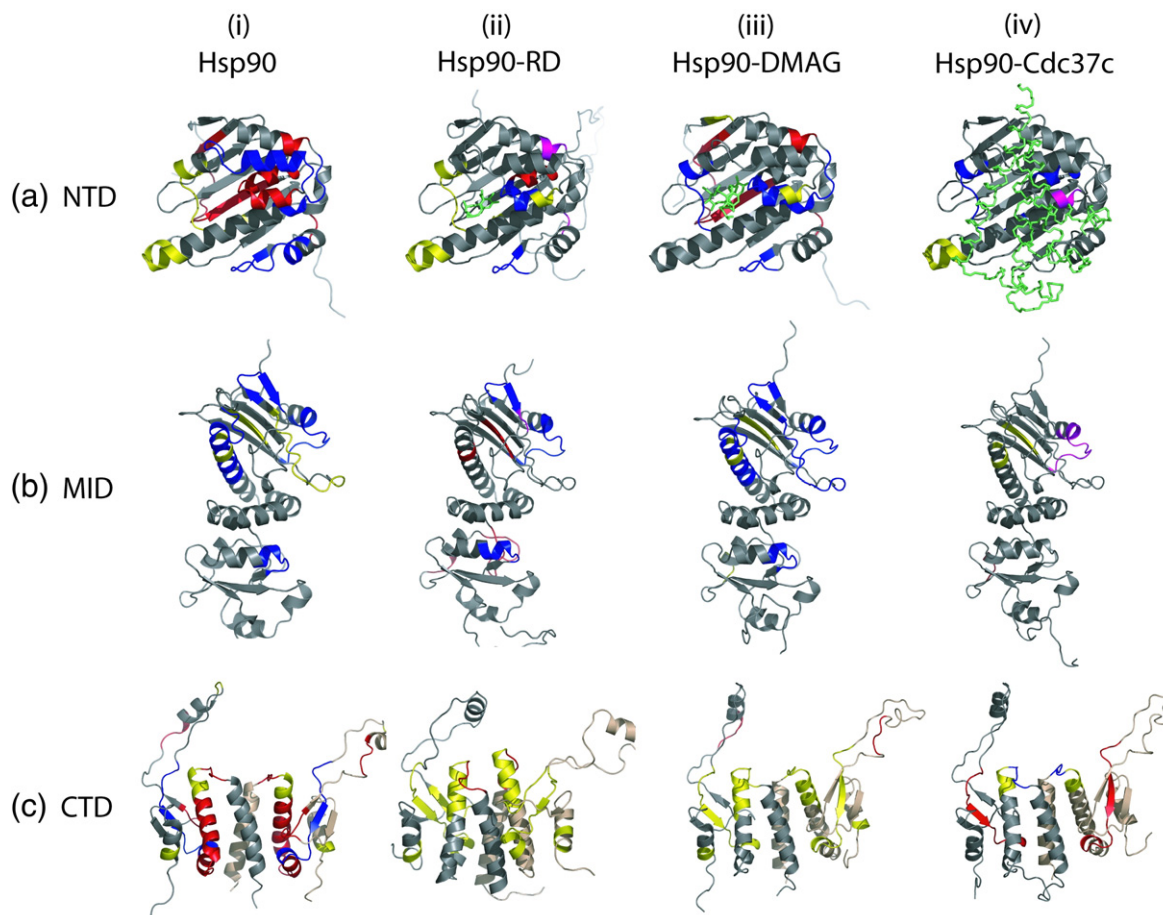
Figure 4. The Hsp90 NTD (a) middle domain (b) and CTD (c) rendered as a cartoon model in grey with peptides coloured according to the slowest observed hydrogen-exchange rate: red, fast; magenta, intermediate; blue, slow. Yellow indicates a peptide that does not undergo any off-exchange over the time-course of the experiment. (i) Apo-Hsp90, (ii) Hsp90-RD, (iii) Hsp90-DMAG and (iv) Hsp90-Cdc37c. The inhibitory ligands and co-chaperone are rendered as stick models in green.

complex. The β13-α11 loop exhibits considerable structural variation in the high-resolution crystal model of yeast Hsp90 middle domain, ranging from disordered to helical.[22] The degree of structure in the catalytic loop is likely enhanced by interaction with the γ-phosphate of ATP in the ATP-bound form where the lid segment has rotated to cover the binding site.[27] Superimposing the structures of a model of the ATP-bound form and the DMAG-NTD complex, the 17' substituent of DMAG is within 3 Å of the γ-phosphate in the equivalent ATP complex (assuming the rotamer that orients towards the middle domain) and is, therefore, able to contact Arg412 in the catalytic loop. Our results suggest that there is an unfavourable interaction between the 17' substituent on DMAG and Arg412 that disrupts structure in the catalytic loop.

There are multiple possible sites of contact between the NTD and middle domains of Hsp90, especially in the eukaryotic homologues that possess an extended (~50 residue) charged-linker region between the domains, which may afford additional conformational flexibility. From our HX-MS data, in addition to the data for the catalytic loop peptide described above, we have two additional

probes in this region, which together indicate a change in the relative positioning of the NTD and middle domain on ligand binding. For example, peptide ion 420.25 is assigned to β11–β12 of the five-stranded sheet in the middle domain, and has four amide groups predicted from the structural model to be available for exchange, the other two participating in β-sheet or β-turn hydrogen-bonding. In free Hsp90, as well as the complexes, these four amide protons on-exchanged with deuterium, however, the degree of off-exchange was halved from two deuterons in the apo-protein to one deuteron in the inhibitor complexes. The reduction in the extent of off-exchange was concomitant with a reduction in the observed fraction of amide deuterons exchanging under a fast-regime. This was tested further directly by inducing off-exchange at a lower temperature (4 °C) (Figure 5(b)). These data fit a structural model in which Tyr376 in β11 in the middle domain is involved in a hydrophobic interaction with Phe228, which is in the slowly exchanging α9-β8 loop in the NTD, upon the formation of the Hsp90-complexes as has been recently described for the p23-yeast Hsp90 complex.[27] In addition, peptide ions 840.42 and 760.85 report on α10, which is packed against the

five-stranded β-sheet of the middle domain and the α10-β9 distal loop (Figure 5(b)). In both the apo-protein and in the Hsp90-ligand complexes, one amide of peptide ion 760.85 exchanged slowly (*t*>30 mins), but the others exchanged at a faster rate in the two Hsp90-complexes compared with the free protein (Figure 5(b)). Additionally, an increase in on-exchange of 1.4 deuterons was observed in the Hsp90-RD complex that was not seen in the Hsp90-DMAG complex. These data indicate a reduction in the higher-order structure in the region of α10 and the following loop upon binding of radicicol (as opposed to an ansamycin) inhibitor ligand to the NTD.

The C-terminal domain

Within the C-terminal domain, two peptides showed significant differences in their hydrogen exchange pattern on complex formation indicative of conformational changes. In both the Hsp90-inhibitor complexes a reduction in total on-exchange and differences in off-exchange pattern, were observed for peptide ions 595.28 and 624.34 (Figure 5(c)). The peptide ion 595.28 was assigned to a short stretch of loop and a peripheral strand in the three-stranded β-sheet. Two amide protons within this peptide on-exchanged with deuterium, but no subsequent off-exchange was observed in the RD-Hsp90 complex. In contrast, in the free dimer, three amide protons in this peptide underwent on-exchange and just one of them exchanged off during the experiment, under a fast regime. This suggests that a single highly exposed amide in the CTD of the free dimer has been rendered completely inaccessible to solvent upon binding of RD to the NTD.

The peptide ion 624.34 shows an even greater contrast in exchange behaviour between the free and RD-bound forms (Figure 5(c)). For the free dimer, five amide groups are shown to have bound deuterium in the on-exchange period (*t*=0 mins) and 1.4 of them exchange off within 30 min (a fast/intermediate exchange regime), with a further amide group off-exchanging under a slow regime overnight at 25 °C. In comparison, in the Hsp90-RD complex this peptide only exchanged three amide protons during the on-labelling period and none of these exchanged back within the time-course of the experiment. This suggests that three amides, within the 14 available for exchange in the 16-mer peptide, become completely protected from solvent upon binding of RD to the NTD. This peptide locates to the central strand of the three-stranded β-sheet and the flanking loop regions, and forms part of the interface with the middle domain in the HtpG molecular envelope[24] and in the crystal structure of an engineered yeast Hsp90 with p23/Sba1.[27] Therefore, these data strongly suggest that there is a tightening of the interaction between the two domains at this location on inhibitor binding, establishing that there is an allosteric effect that spans 90 Å upon binding of a small molecule inhibitor to the N-terminal ATP-binding site.

The results for the Hsp90-DMAG complex were in qualitative agreement with the Hsp90-RD results for the CTD presented above (Figure 5(c)).

The results of the H/D exchange experiments on the two Hsp90-inhibitor complexes, in which the small molecules DMAG and RD are bound to the ATP-binding site in the NTD, are in good agreement, suggesting that the different classes of inhibitor induce similar conformational changes. Both inhibitors change the amide group protection of peptides in all three structured domains of Hsp90, demonstrating that there are long-range effects of inhibitor binding thath are not picked up in the crystal structures of the complexed N-terminal domain alone.

In the NTD, differences are seen in the lid-segment of the ATP-binding site (helices α5, α6 and α7), at the C terminus of α2 through to α3 and at the C terminus of strand β3, the helix α4 and the intervening β3-α4 loop (Figure 5(a)). In the middle domain, differences in amide protection are observed in the α10-β9 loop, in the five-stranded β-sheet (strands β11 and β12) and at the N terminus of α11 and the preceding β13-α11 loop (Figure 5(b)). Data for the Hsp90-RD complex indicate two spatially adjacent peptides within the CTD that are protected relative to the free protein, corresponding to β18, β19 and α20 (Figure 5(c)). The same pattern of protection is observed in the Hsp90-DMAG complex, however, the reduction in exchangeable amide groups is not as pronounced as with Hsp90-RD.

Conformational changes in Hsp90 upon co-chaperone binding

HX-MS experiments were also undertaken for the complex between Hsp90 and the co-chaperone Cdc37c, and the results are shown in Figures 4 and 5. Regions of Hsp90 that show significant differences in their H/D exchange patterns and/or rates on Cdc37c binding, indicative of conformational change, are discussed in detail below domain by domain.

The N-terminal-binding domain

A crystal structure for the complex formed between the NTD of yeast Hsp90 and the CTD of human Cdc37 has been solved.[32] The structure indicates that the predominant contact surface between the two proteins is the lid-segment of Hsp90 (residues 128–150 in human Hsp90). In addition, there is a conserved interaction between Arg167 of Cdc37 and Glu62 in α2 of Hsp90.

The HX-MS data for the Hsp90-Cdc37c complex presented here reveal both structural effects expected and in keeping with the crystal structure for the complex formed between the isolated Hsp90-NTD and Cdc37c domains,[32] as well as, additional changes evident only in this study of full-length Hsp90 in solution.

In keeping with the high-resolution crystal structure, the Hsp90-Cdc37c complex shows evidence of a slight structural alteration at the tip of the lid segment relative to free Hsp90: the peptide ion 350.22

(residues 143–145) shows very rapid off-exchange of 0.5 deuterons (<1 min) in free Hsp90, yet exchanges off slowly (>30 min) in the presence of Cdc37c. Notably, the degree of on-exchange of this peptide was greatest in the Hsp90-Cdc37c complex (1.6 deuterons), although the number of amides that were able to off-exchange was identical between all of the states of Hsp90 (apo-protein and complexes). Two other slight changes in the HX-MS profile were observed for peptides in the NTD upon binding of Cdc37c. These are located in regions that are unperturbed in the crystal structure of Cdc37c-Hsp90 complex relative to free Hsp90-NTD. Peptide ion 776.46 was assigned to a heptapeptide in β8 of the eight-stranded β-sheet and, although detectable

exchange was observed for only three of the five amides, there was a distinct reduction in the off-exchange rate of one amide group in the peptide when Cdc37c was bound (Figure 5(a)). The peptide ion 535.37 also showed enhanced protection in the complex (a single amide that exchanged slowly in free Hsp90 exhibited no off-exchange when Cdc37c was bound) (Figure 5(a)). This peptide, located at the C terminus of α3 and the subsequent α3-β2 loop, is spatially close to peptide ion 776.46.

The middle domain

Two peptide ions, 420.25 and 393.28, assigned to peptides in the middle domain, showed alterations in
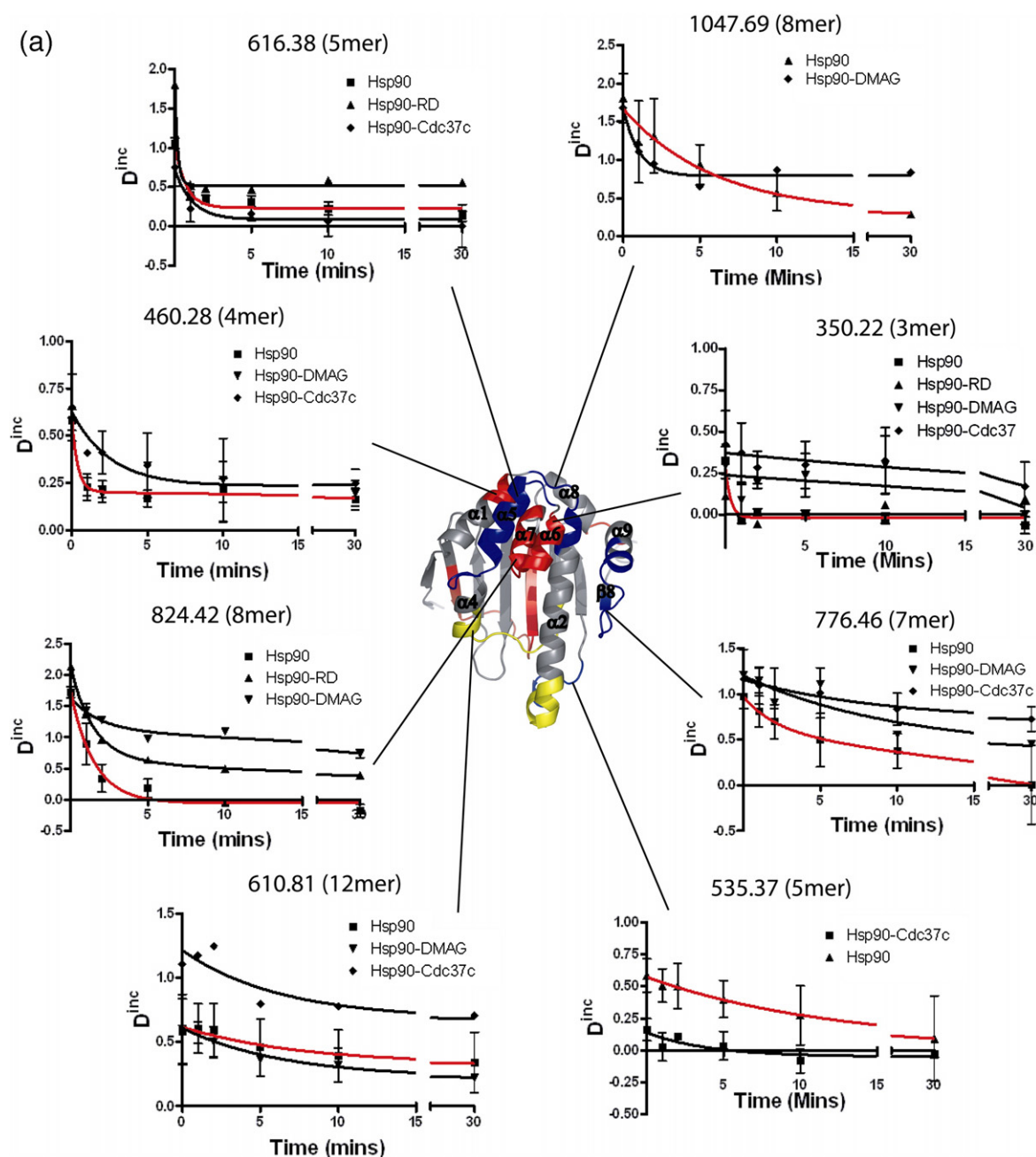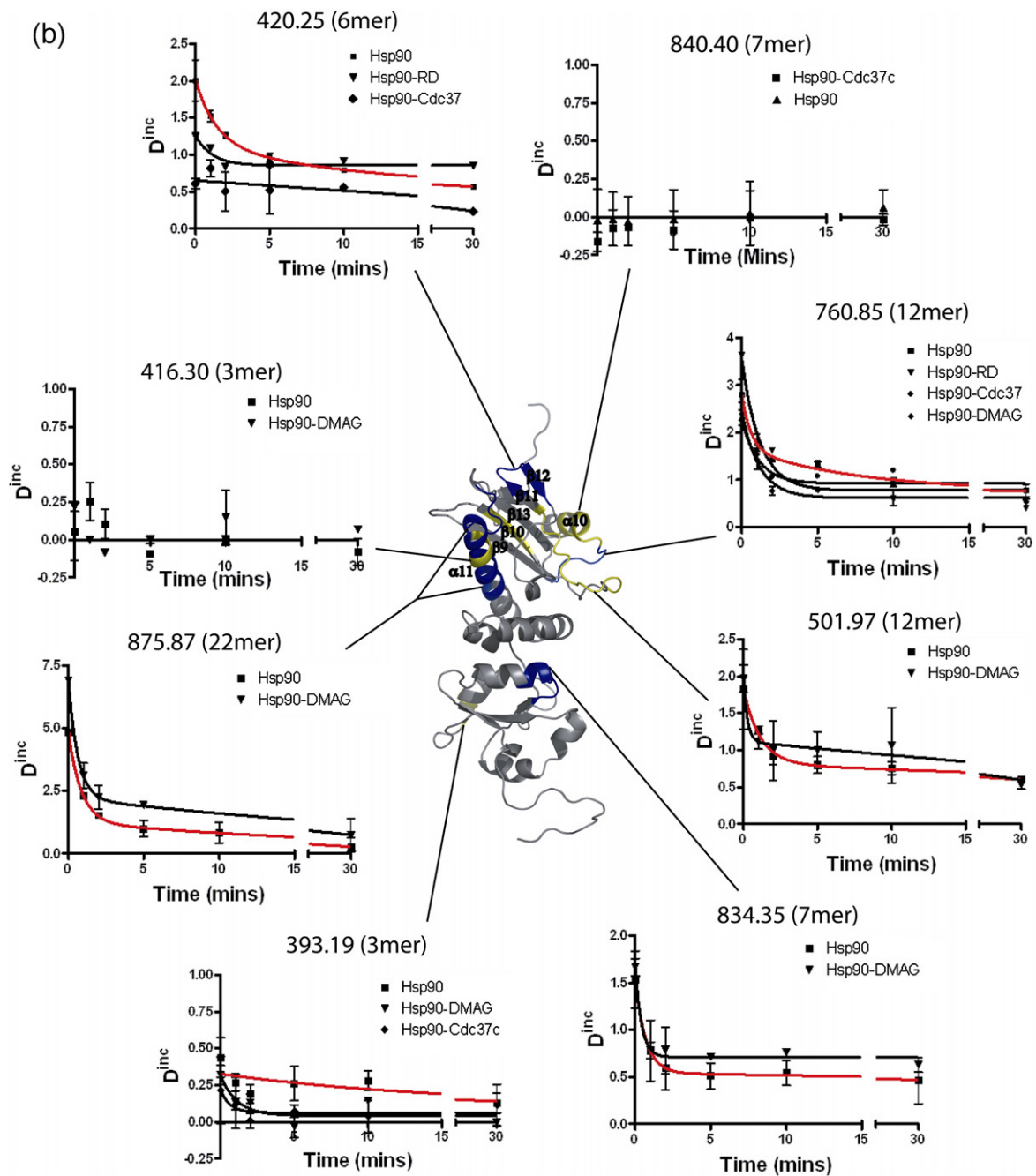

Figure 5 (*legend on page 1198*)

Figure 5 (*legend on next page*)

HX-MS off-exchange rate when Cdc37c was bound to Hsp90. The peptide corresponding to the ion at 420.25 *m/z* is located in the middle domain, spatially adjacent to the NTD. There is a reduction in on-exchange of 1.4 deuterons in this peptide on Cdc37c binding, and no change in off-exchange. These results suggest that this region becomes more stable, and may be more structured, in the complex, thereby reducing local fluctuations that would normally lead to amide exchange. It is interesting to note that these are the same changes observed in the two Hsp90-inhibitor complexes that were attributed to an interaction between Tyr376 in β11 in the middle domain and Phe228, located in the β8 strand in the NTD. These results are inconsistent with the Hsp90-Cdc37c complex adopting the same structure as for that observed for NTD and middle domain of HtpG.[25]

C-terminal domain

No differences were observed in the exchange behaviour for peptides in the CTD between the apo-Hsp90 and the Hsp90-Cdc37c complex. We attribute this, in part, to the fact that the peptide coverage in the CTD for the Hsp90-Cdc37c complex is poor compared to the apo-protein.

As with the studies on the Hsp90-inhibitor complexes, conformational changes on binding of Cdc37c
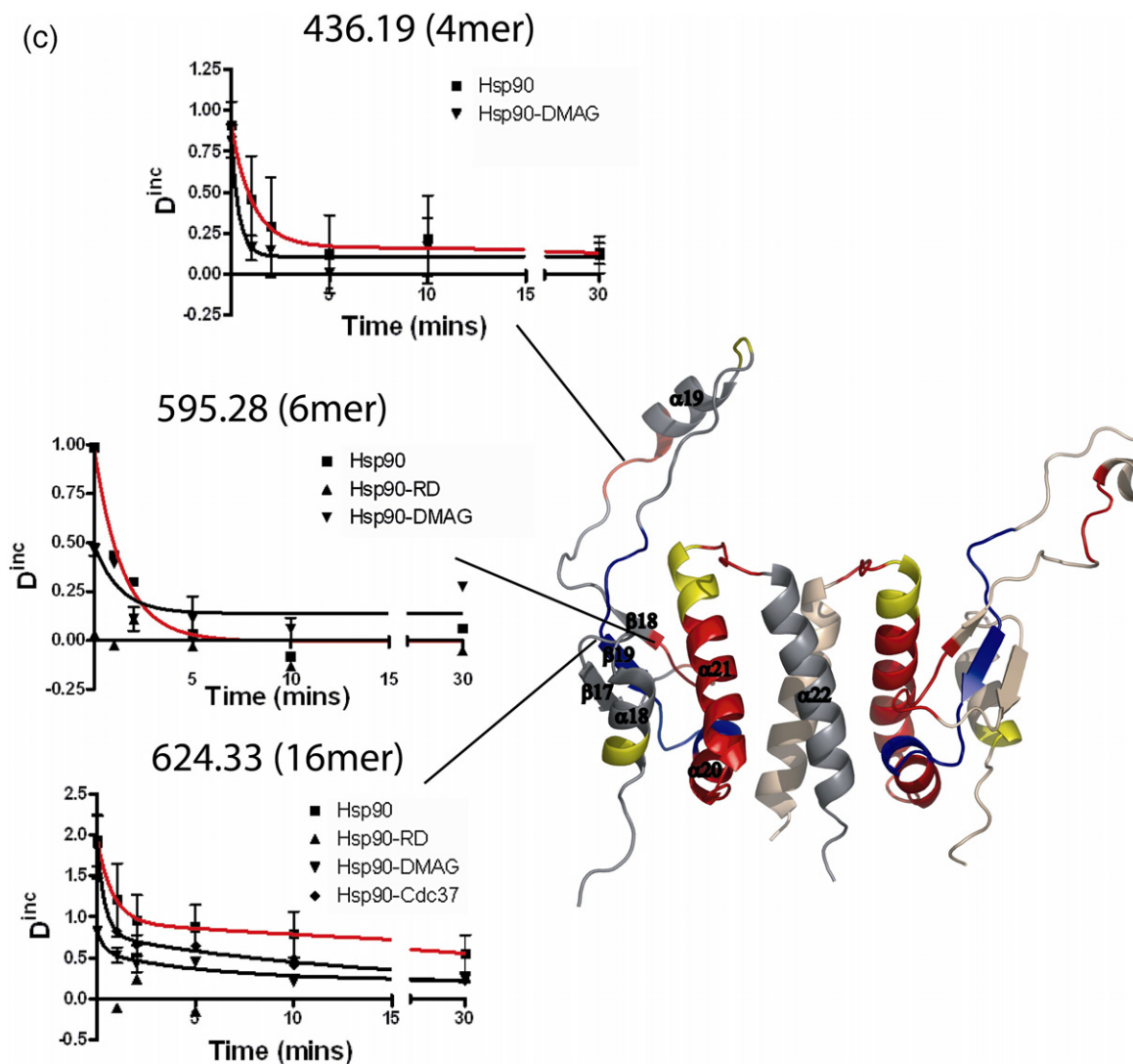
Figure 5. The effect of inhibitors and Cdc37c binding to Hsp90. (a) The Hsp90β-NTD. (b) The Hsp90β-middle domain. (c) The Hsp90β-CTD. Peptides are coloured according to HX-MS rate regime: red, fast; magenta, intermediate; blue, slow; yellow, no-exchange; and grey, no coverage. Normalised off-exchange rate data of exchangeable amides are provided and are linked to the relevant peptides in the structure.

to the NTD remote from the binding site were observed, suggesting long-range allosteric effects.

Global structure of the Hsp90 complexes

Over the years, the relative orientation of the three structural domains of Hsp90, as well as the positioning of the two monomers within the dimer relative to each other, has been the subject of some speculation. Despite recent high-resolution crystal structures of an engineered variant of full-length yeast Hsp82 in complex with the co-chaperone, sba1/p23[27] and a number of structures of the *E. coli* homologue HtpG[25,26] questions on the global structure remain, particularly the structure in solution. Some significant differences between the relative orientations of the NTD and middle domains in these structures were observed, and it is not yet known whether these are due to crystal contacts, the presence of the CTD

and a co-chaperone in one structure, or intrinsic differences between the yeast and *E. coli* homologues. Our hydrogen-exchange data provide valuable information on the structure of full-length human Hsp90 in solution.

The hydrogen-exchange data for Hsp90 complexes presented here show an alteration in the conformational state of the N-terminal domain relative to the middle domain and also a shift in the interaction surface between the CTD and the middle domain on complexation with inhibitors and co-chaperones. Although it has been suggested that the orientation of the NTD and middle domains in the crystal structure of the NTD and middle domains of HtpG are incorrect and due to a crystallographic artefact,[27] our HX-MS data on full-length apo-Hsp90 provide support for the HtpG model.[25] Although we have evidence from SAXS experiments that apo Hsp90 is conformationally dynamic,[6] our HX-MS data sug-
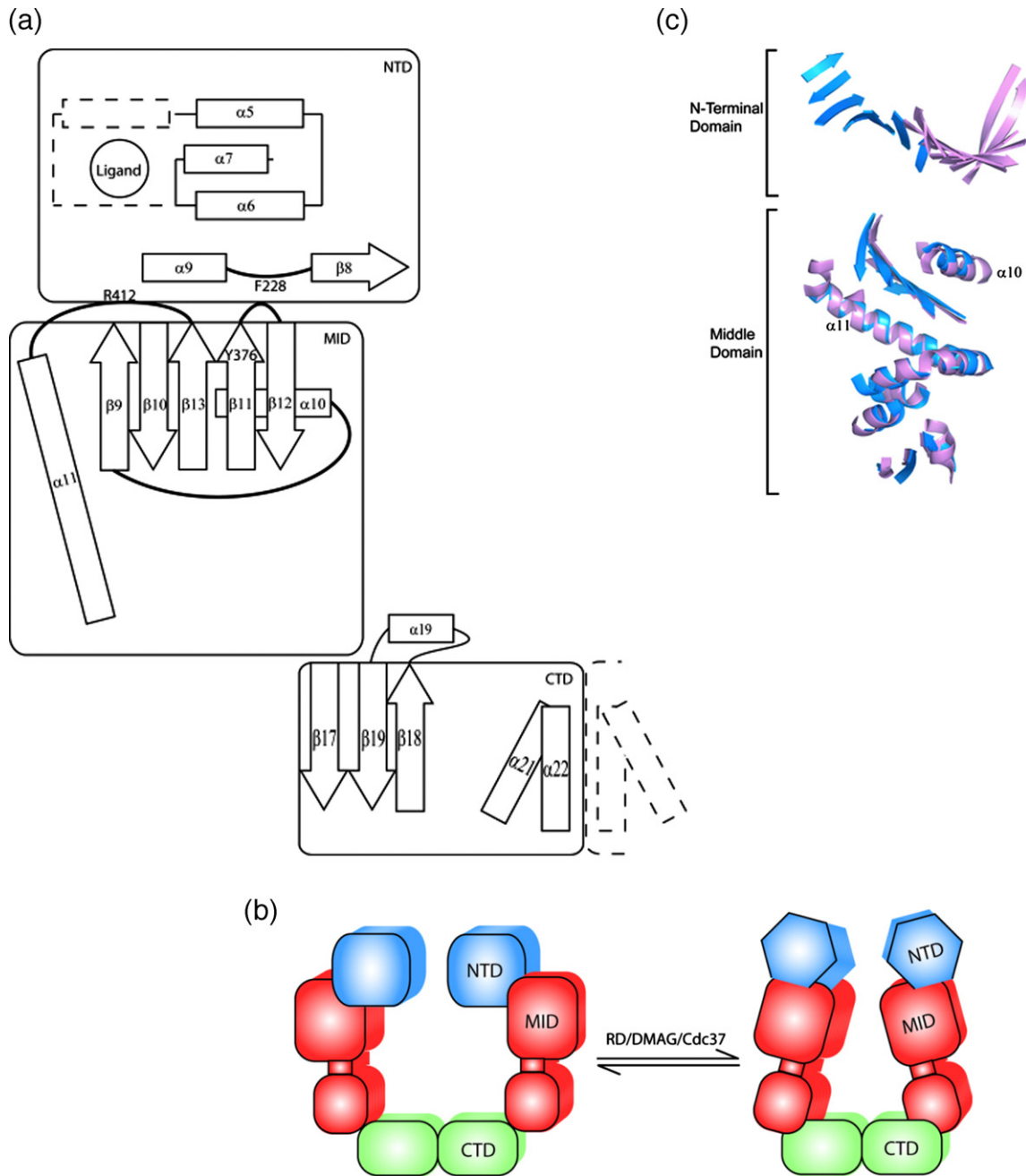
(a)

(c)

(b)

Figure 6. Schematic of the structures that Hsp90 can adopt. (a) Schematic of the structure of Hsp90 showing the three main domains: NTD (blue), MD (red) and CTD (yellow) with some of the important secondary structural elements. Broken lines represent the orientation of the lid-segment in the "closed" conformation. (b) Model for the Hsp90 conformation upon RD/DMAG/Cdc37c binding. There is no evidence for dimerisation of the N-terminal domains in these complexes from our H/D exchange data (data not shown). (c) Detailed structure of the rotation of the NTD relative to the middle domain of $\sim 80°$ observed in the structures of yeast Hsp90 (blue) and HtpG (pink).

gest an orientation in which the α10 helix and α10-β9 distal loop in the middle domain are protected from solvent through an interaction with the NTD, most likely with helix α2, similar to that observed in the HtpG crystal structure.[25]

In contrast, our HX-MS data clearly show that there is another conformational state that is stabilised by the binding of inhibitory ligands such as RD and DMAG or co-chaperones such as Cdc37 to the NTD of Hsp90. In this case, the binding event stabilises a

conformation of Hsp90 in which the NTD and middle domain have rotated relative to each other and our data are most consistent with the orientation shown in the recent crystal structure of the full-length Hsp82 in complex with sba1/p23.[27] There is an approximately 80° rotation of the NTD in the plane of the eight-stranded β-sheet in HtpG (both ADP-bound and apo-forms) relative to Hsp82 (in complex with Sba1/ADP-PNP), MutL and GyrB (Figure 6(b) and (c)). In the complexes of Hsp90 with the small-molecule inhibi-

tory ligands RD and DMAG, a conformational state is trapped in which amides in α10 and α10-β9 are deprotected, and in which the catalytic loop (β13-α11) and Aha1-binding site (α11) become less structured, presumably as a result of the interaction of the middle domain with the liganded NTD (Figure 6(a)). These two sites in the middle domain appear to be mutually exclusive in their interaction with the NTD (Figure 6(c)). Although it seems that the specific state adopted by Hsp90-Cdc37c is not the same as that of Hsp90-RD/DMAG, considering that the Hsp90-inhibitor complexes show reduced radius of gyration by SAXS,[6] whereas the Hsp90-Cdc37 complex shows an extended structure by EM in the presence of a client protein,[34] there are clearly some structural features in common, as indicated by our HX-MS data.

Our data on both free and complexed Hsp90 are consistent with two different conformational states where the relative populations are influenced by ligand binding to the NTD (Figure 6(b)). Cdc37c binding cannot occur in the proposed apo-conformation of Hsp90, due to steric clashes between the middle domain and the co-chaperone. The co-chaperone-bound conformation involves a stable interaction between α9-β8 in the NTD and β11 in the middle domain, in which the NTD is rotated relative to the middle domain to create a more extended structure (Figure 6(a) and (b)). This extended structure has also been experimentally observed and documented by Vaughan *et al.* in a complex of yeast Hsp90 with Cdc37 and Cdk4.[34] Binding of inhibitory ligands results in a restructuring of the catalytic loop region. Key interactions between the N-terminal and middle domains appear to be shared between the Hsp90-RD, Hsp90-DMAG and Hsp90-Cdc37c complexes, giving rise to the suggestion of a potential co-operative model for binding of ligand and co-chaperone. This may explain the different affinities for drugs observed *in vitro* and *in vivo* and in different cell types.

We rationalise the HX-MS data within a model for Hsp90 action similar to that postulated by Shiau *et al.* in which RD/DMAG-binding to the NTD is incompatible with the relative domain orientation in the apo and ATP-bound forms and results in the stabilisation of a condensed form.[26] It is this condensed form that they claim is the ADP-bound state. Liganded ADP, lacking a γ-phosphate, is unable to stabilise an interaction with R410 (R380 in *S. cerevisiae* and R336 in *E. coli*) in the catalytic loop located in the middle domain and also has been shown to disrupt the local structure of the NTD lid-segment.[25,26] Similarly, liganded RD cannot make a stable interaction with R410 and DMAG makes an unfavourable interaction with the catalytic loop and Aha1 binding site. Both inhibitors seem to have little impact on the degree of solvent exposure in the lid-segment, therefore, it is likely that they exert their long-range allosteric effects through a subtly different mechanism than ADP. Both inhibitors induce N-terminal domain rotation and re-orientation relative to the MD, as does ADP, however, the allosteric mechanism remains highly unclear: it may be dependent upon local structural rearrangements within each monomer, likely transmitted through the MD by means of a "hinge" between the two α-β-α subdomains by flexing around α11–α12–α13, or it could be due to a domain-swap cyclised structure as proposed by Agard and co-workers.[26]

In conclusion, using pepsin digestion of the Hsp90 dimer and MS-MS techniques, we have been able to assign 72 peptide ions resulting in some 68% coverage of the structured domains of Hsp90. Combining this with H/D-exchange for apo and complexed Hsp90, we have been able to obtain structural information on the conformational changes induced in Hsp90 on binding of inhibitor ligands or a co-chaperone, representing one of the largest systems to date that has been analysed by the HX-MS approach. This investigation, characterising the structural changes in full-length dimeric Hsp90 in solution on complexation, complements other structural work in the field that has examined either isolated domains or full-length Hsp90 in a crystalline form.

Here, we have presented evidence for long-range changes in conformation of Hsp90 on both inhibitor and co-chaperone binding to the N-terminal domain. Changes in the pattern and rate of H/D exchange are observed not only in the NTD but in the middle and C-terminal domains. On the binding of RD and DMAG we rationalise the results as a stabilisation of a particular conformational state in which there has been a change (possibly tightening) in the interaction between the C-terminal and middle domains, and a change in interface between NTD and middle domain, from one involving α10-β9 to one involving the catalytic loop and β11–β12. This is qualitatively consistent with our previous SAXS results in which we observed a reduction in the radius of gyration on inhibitor binding. We suggest that RD and DMAG binding to Hsp90 cause it to adopt a structure where the domains are more tightly packed and have reduced conformational freedom, with significant changes to the spatial locations and quaternary arrangement of the structured domains and the interfaces that join them.

Experimental Procedures

Protein expression and purification

Human Hsp90β and Cdc37c were expressed and purified as described.[6,7]

Structural modelling of human Hsp90β

Alignment of multiple protein sequences was done using the Clustal W algorithm with subsequent manual editing.[35] Proteins were structurally aligned with ALIGN3D and modelled using Modeller.[36] The stereochemical integrity of the models was assessed with Procheck[37] and the molecular energy was assessed with Prosa2003.[38] Templates used were 1sf8 for the C-terminal domain, 1hk7 for the middle domain and 1yet, 1yes, 1osf, 1bgq and 1us7 for the various forms of the N-terminal domain.

Hydrogen-exchange

All labile hydrogen atoms in the protein samples were initially replaced with deuterium atoms. This procedure, along with desalting, concentrating, as well as buffer exchange, was carried out using Vivaspin500R filters (Sartorius, DE). A 5 kDa cut-off filter was used for Cdc37c and a 50 kDa filter for Hsp90. Each solution was typically washed twice in aqueous ammonium acetate buffer for desalting and buffer exchange (20 min for each cycle) at 4 °C and subsequently three times with deuterated ammonium acetate in ^2H_2O for complete deuteration (30 min for each cycle) at 4 °C. The small-molecule inhibitory ligands were lyophilised and resuspended in deuterated ammonium acetate buffer with ^2H_2O and D$_6$-DMSO as required. Aliquots of each solution of deuterated Hsp90 and ligand sample were then mixed to form the complex. To ensure that Hsp90 was essentially 100% bound in solution the molar ratios of protein:ligand were 1:9 for Hsp90:GA (assuming a K_d of 1.1 μM by intrinsic fluorescence, unpublished data), 1:2 for Hsp90:RD (assuming a K_d of 19 nM[21]), 1:1.5 for Hsp90:DMAG (assuming a K_d of 0.5 μM) and 1:2.5 for Hsp90:Cdc37c (assuming a K_d of 3.8 μM[6]). The sample solutions containing the complexes were incubated at 4 °C overnight to allow complete deuteration and equilibration of complex. Hydrogen exchange was then initiated at room temperature by a 1:10 dilution with 25 mM or 250 mM aqueous ammonium acetate (unless specified in the text). The concentration of Hsp90 was typically around 25 μM after dilution. At various times, an aliquot of the solution was removed and the exchange quenched by addition of acetic acid to reduce the pH to 2.7 (pH meter tested). The aliquot was digested for 5 min at 4 °C with an equal volume of 2 mg ml^{-1} aqueous pepsin solution and then loaded into a mounted nanoelectrospray needle that was pre-chilled to −20 °C and analysed directly by mass spectrometry (estimated dead time ~30 s).

Mass spectrometry data acquisition

Hydrogen exchange measurements and MS/MS of peptic peptides were carried out on a Q-Tof1 mass spectrometer (Waters, UK). Samples were introduced into the spectrometers *via* gold-coated nano-electrospray needles, prepared in the laboratory.[39] The instruments were calibrated using 100 mg ml^{-1} aqueous CsI. For localisation of hydrogen exchange in pepsin-digested Hsp90 samples, typical instrumental settings include: mass range 200–2000 Da, capillary voltage 1400 V and cone voltage 20 V. Source temperature and desolvation temperature were both set at room temperature. The data acquired in the first minute were used for analysis.

Peptide sequence assignment

50 μM protein in 21 mM ammonium acetate was mixed with 100% acetic acid in a 10:1 ratio (v/v) and digested for 5 min at 4 °C with an equal volume of 2 mg ml^{-1} aqueous pepsin solution. The sample was analysed directly by nanoESI-MS/MS with a Micromass Q-Tof1 mass spectrometer. The Hexapole collision cell was supplied with Ar gas at a pressure of 2.5 psi. Each selected ion was isolated by adjustment of the LM Resolution and HM Resolution around the target *m/z*. The collision energy

was increased stepwise until base peak intensity was reduced by 75%. Spectra were acquired for a minimum of 1 min.

Analysis of mass spectrometry data

Mass spectrometry data were processed using Masslynx (Waters, UK), Excel (Microsoft, US) and Prism4 (Graphpad, US). The centroid (M) of the isotope envelope of each peptic peptide was calculated manually by the following equation:[40]

$$M = \sum (m_i I_i) / \sum I_i$$

where m_i and I_i are the mass and relative abundance of the isotope peak, respectively, in an isotope envelope. Deuterons retained (D_{inc}) of each peptide were calculated from the following equation:

$$D_{inc} = (M - M_{min})$$

where M_{min} is the centroid of the labelled peptide after overnight off-exchange, i.e. the minimum value of the centroid that was observed experimentally. Therefore, D_{inc} represents only the deuterons that were off-exchanged within the timescale of the experiment and does not include a back-exchange correction. The retained exchangeable deuterons were plotted against exchange time for individual peptides.

Chemicals and reagents

All chemicals were of analytical or mass spectrometric grade. Pepsin, ammonium acetate and deuterated DMSO were obtained from Sigma, deuterium oxide (^2H_2O, >99.96%) was obtained from Aldrich and deuterated ammonium acetate (>99%) from Gross Scientific Instruments Ltd.

References

1. Picard, D. (2002). Heat-shock protein 90, a chaperone for folding and regulation. *Cell. Mol. Life Sci.* **59**, 1640–1648.
2. Zhao, R. M., Davey, M., Hsu, Y. C., Kaplanek, P., Tong, A., Parsons, A. B. *et al.* (2005). Navigating the chaperone network: an integrative map of physical and genetic interactions mediated by the Hsp90 chaperone. *Cell*, **120**, 715–727.
3. Buchner, J. (1999). Hsp90 and Co.- a holding for folding. *Trends Biochem. Sci.* **24**, 136–141.
4. Wegele, H., Wandinger, S. K., Schmid, A. B., Reinstein, J. & Buchner, J. (2006). Substrate transfer from the chaperone Hsp70 to Hsp90. *J. Mol. Biol.* **356**, 802–811.
5. Panaretou, B., Prodromou, C., Roe, S. M., O'Brien, R.,

Ladbury, J. E., Piper, P. W. & Pearl, L. H. (1998). ATP binding and hydrolysis are essential to the function of the Hsp90 molecular chaperone *in vivo. EMBO. J.* **17**, 4829–4836.

6. Zhang, W., Hirshberg, M., McLaughlin, S. H., Lazar, G. A., Grossmann, J. G., Nielsen, P. R. *et al.* (2004). Biochemical and structural studies of the interaction of Cdc37 with Hsp90. *J. Mol. Biol.* **340**, 891–907.

7. McLaughlin, S. H., Smith, H. W. & Jackson, S. E. (2002). Stimulation of the weak ATPase activity of human Hsp90 by a client protein. *J. Mol. Biol.* **315**, 787–798.

8. McLaughlin, S. H., Sobott, F., Yao, Z. P., Zhang, W., Nielsen, P. R., Grossmann, J. G. *et al.* (2006). The co-chaperone p23 arrests the Hsp90 ATPase cycle to trap client proteins. *J. Mol. Biol.* **356**, 746–758.

9. Prodromou, C., Siligardi, G., O'Brien, R., Woolfson, D. N., Regan, L., Panaretou, B. *et al.* (1999). Regulation of Hsp90 ATPase activity by tetratricopeptide repeat (TPR)-domain co-chaperones. *EMBO J.* **18**, 754–762.

10. Panaretou, B., Siligardi, G., Meyer, P., Maloney, A., Sullivan, J. K., Singh, S. *et al.* (2002). Activation of the ATPase activity of Hsp90 by the stress-regulated cochaperone Aha1. *Mol. Cell*, **10**, 1307–1318.

11. Siligardi, G., Panaretou, B., Meyer, P., Singh, S., Woolfson, D. N., Piper, P. W. *et al.* (2002). Regulation of Hsp90 ATPase activity by the co-chaperone Cdc37p/p50(cdc97). *J. Biol. Chem.* **277**, 20151–20159.

12. Miyata, Y. (2005). Hsp90 inhibitor geldanamycin and its derivatives as novel cancer chemotherapeutic agents. *Curr. Pharm. Des.* **11**, 1131–1138.

13. Moulin, E., Zoete, V., Barluenga, S., Karplus, M. & Winssinger, N. (2005). Design, synthesis, and biological evaluation of HSP90 inhibitors based on conformational analysis of radicicol and its analogues. *J. Am. Chem. Soc.* **127**, 6999–7004.

14. Wright, L., Barril, X., Dymock, B., Sheridan, L., Surgenor, A., Beswick, M. *et al.* (2004). Structure-activity relationships in purine-based inhibitor binding to HSP90 isoforms. *Chem. Biol.* **11**, 775–785.

15. Workman, P. (2004). Combinatorial attack on multi-step oncogenesis by inhibiting the Hsp90 molecular chaperone. *Cancer Letters*, **206**, 149–157.

16. Workman, P. (2004). Altered states: selectively drugging the Hsp90 cancer chaperone. *Trends Mol. Med.* **10**, 47–51.

17. Grem, J. L., Morrison, G., Guo, X. D., Agnew, E., Takimoto, C. H., Thomas, R. *et al.* (2005). Phase I and pharmacologic study of 17-(allylamino)-17-demethoxygeldanamycin in adult patients with solid tumors. *J. Clin. Onco.* **23**, 1885–1893.

18. Prodromou, C., Roe, S. M., Piper, P. W. & Pearl, L. H. (1997). A molecular clamp in the crystal structure of the N-terminal domain of the yeast Hsp90 chaperone. *Nature Struct. Biol.* **4**, 477–482.

19. Prodromou, C., Roe, S. M., O'Brien, R., Ladbury, J. E., Piper, P. W. & Pearl, L. H. (1997). Identification and structural characterization of the ATP/ADP-binding site in the Hsp90 molecular chaperone. *Cell*, **90**, 65–75.

20. Stebbins, C. E., Russo, A. A., Schneider, C., Rosen, N., Hartl, F. U. & Pavletich, N. P. (1997). Crystal structure of an Hsp90-geldanamycin complex: targeting of a protein chaperone by an antitumor agent. *Cell*, **89**, 239–250.

21. Roe, S. M., Prodromou, C., O'Brien, R., Ladbury, J. E., Piper, P. W. & Pearl, L. H. (1999). Structural basis for inhibition of the Hsp90 molecular chaperone by the antitumor antibiotics radicicol and geldanamycin. *J. Med. Chem.* **42**, 260–266.

22. Meyer, P., Prodromou, C., Hu, B., Vaughan, C. K., Roe, S. M., Panaretou, B. *et al.* (2003). Structural and functional analysis of the middle segment of Hsp90: implications for ATP hydrolysis and client protein and cochaperone interactions. *Mol. Cell*, **11**, 647–658.

23. Meyer, P., Prodromou, C., Liao, C. Y., Hu, B., Roe, S. M., Vaughan, C. K. *et al.* (2004). Structural basis for recruitment of the ATPase activator Aha1 to the Hsp90 chaperone machinery. *EMBO J.* **23**, 511–519.

24. Harris, S. F., Shiau, A. K. & Agard, D. A. (2004). The crystal structure of the carboxy-terminal dimerization domain of HtpG, the *Escherichia coli* Hsp90, reveals a potential substrate binding site. *Structure*, **12**, 1087–1097.

25. Huai, Q., Wang, H. C., Liu, Y. D., Kim, H. Y., Toft, D. & Ke, H. M. (2005). Structures of the N-terminal and middle domains of *E.coli* Hsp90 and conformation changes upon ADP binding. *Structure*, **13**, 579–590.

26. Shiau, A. K., Harris, S. F., Southworth, D. R. & Agard, D. A. (2006). Structural analysis of *E.coli* hsp90 reveals dramatic nucleotide-dependent conformational rearrangements. *Cell*, **127**, 329–340.

27. Ali, M. M. U., Roe, S. M., Vaughan, C. K., Meyer, P., Panaretou, B., Piper, P. W. *et al.* (2006). Crystal structure of an Hsp90-nucleotide-p23/Sba1 closed chaperone complex. *Nature*, **440**, 1013–1017.

28. Pearl, L. H. & Prodromou, C. (2006). Structure and mechanism of the Hsp90 molecular chaperone machinery. *Annu. Rev. Biochem.* **75**, 271–294.

29. Pearl, L. H. & Prodromou, C. (2000). Structure and in vivo function of Hsp90. *Curr. Opin. Struct. Biol.* **10**, 46–51.

30. Richter, K., Moser, S., Hagn, F., Friedrich, R., Hainzl, O., Heller, M. *et al.* (2006). Intrinsic inhibition of the Hsp90 ATPase activity. *J. Biol. Chem.* **281**, 11301–11311.

31. McLaughlin, S. H., Ventouras, L. A., Lobbezoo, B. & Jackson, S. E. (2004). Independent ATPase activity of Hsp90 subunits creates a flexible assembly platform. *J. Mol. Biol.* **344**, 813–826.

32. Roe, S. M., Ali, M. M. U., Meyer, P., Vaughan, C. K., Panaretou, B., Piper, P. W. *et al.* (2004). The mechanism of Hsp90 regulation by the protein kinase-specific cochaperone p50(cdc37). *Cell*, **116**, 87–98.

33. Jez, J. M., Chen, J. C. H., Rastelli, G., Stroud, R. M. & Santi, D. V. (2003). Crystal structure and molecular modeling of 17-DMAG in complex with human Hsp90. *Chem. Biol.* **10**, 361–368.

34. Vaughan, C. K., Gohlke, U., Sobott, F., Good, V. M., Ali, M. M. U., Prodromou, C. *et al.* (2006). Structure of an Hsp90-Cdc37-Cdk4 complex. *Mol. Cell*, **23**, 697–707.

35. Thompson, J. D., Higgins, D. G. & Gibson, T. J. (1994). CLUSTAL-W- Improving the sensitivity of progressive multiple sequence alignment through sequence weighting, position-specific gap penalties and weight matrix choice. *Nucl. Acid Res.* **22**, 4673–4680.

36. Fiser, A. S. & Sali, A. (2003). MODELLER: generation and refinement of homology-based protein structure models. *Macromol. Cryst. Part D, Methods Enz.* **374**, 461.

37. Laskowski, R. A., Macarthur, M. W., Moss, D. S. & Thornton, J. M. (1993). PROCHECK - a program to check the stereochemical quality of protein structures. *J. Appl. Crystallog.* **26**, 283–291.

38. Sippl, M. J. (1993). Recognition of errors in 3-dimensional structures of proteins. *Proteins: Struct. Funct. Genet.* **17**, 355–362.

39. Nettleton, E. J., Sunde, M., Lai, Z. H., Kelly, J. W., Dobson, C. M. & Robinson, C. V. (1998). Protein subunit interactions and structural integrity of amyloidogenic transthyretins: evidence from electrospray mass spectrometry. *J. Mol. Biol.* **281**, 553–564.

40. Lam, W. & Ramanathan, R. (2002). In electrospray ionization source hydrogen/deuterium exchange LC-MS and LC-MS/MS for characterization of metabolites. *J. Am. Chem. Soc.* **13**, 345–353.

Edited by M. Gottesman